Reactions of Laser-Ablated U and Th with CO_2: Neon Matrix Infrared Spectra and Density Functional Calculations of OUCO, OThCO, and Other Products

Lester Andrews,*,† Mingfei Zhou,† Binyong Liang,† Jun Li,‡ and Bruce E. Bursten*,‡

Contribution from the Department of Chemistry, University of Virginia, Charlottesville, Virginia 22904-4319, and the Department of Chemistry, The Ohio State University, Columbus, Ohio 43210

Received May 15, 2000

Abstract: Laser-ablated U and Th atoms react with CO_2 to give OUCO (1806.9, 823.2 cm^{-1}) and OThCO (1778.4 cm^{-1}) as major products, which are identified by isotopic substitution ($^{13}CO_2$, $C^{18}O_2$ and $^{12}CO_2 + {}^{13}CO_2$, $C^{16}O^{18}O + C^{18}O_2$ mixtures), doping with CCl_4 as an electron trap, and comparison with frequencies from density functional calculations. The insertion reaction is spontaneous as these bands increase on annealing the neon matrix from 4 to 6 K. Further reaction of OAnCO (An = Th, U) with another CO_2 molecule gives the $O_2An(CO)_2$ product, although much more so with uranium than thorium. Reaction of the metal cations with CO_2 produces $OUCO^+$ (2073.0, 881.2 cm^{-1}) and $OThCO^+$ (2009.9, 896.4 cm^{-1}) with higher yield in thorium experiments. The $O_2An(CO)_2^-$ anions are observed for both metals again with higher yield in uranium investigations.

Introduction

Carbon dioxide is a major source of atmospheric carbon and one of the largest carbon stocks on our planet. The possibility of using CO_2 to synthesize useful chemical compounds has been actively explored.[1−5] Because of its large C═O bond energy, CO_2 is a thermodynamically stable molecule that needs to be activated via bonding interactions with metal centers. The reaction of CO_2 with thermal first-row transition-metal atoms has been investigated both experimentally[6−9] and theoretically,[10−14] and this work has already been reviewed.[15] Recent reactions of laser-ablated transition-metal atoms with CO_2 give primarily the insertion product, OMCO, while photoisomerization and photoionization processes do occur for certain metals and wavelengths.[16−21] For several heavier metals the $O_2M(CO)_2$ reduction product has also been characterized.[17,21]

While recent experimental and theoretical investigations of carbon dioxide complexes of transition metals have revealed intriguing chemistry, little work has been done with actinide metals and CO_2.[22] The only work in this field is an argon matrix study with uranium that revealed spectra for the OUCO and O_2UCO molecules,[23] which are in good agreement with the neon matrix spectrum reported here. In our laboratories, we have systematically investigated the reactions between thorium/uranium and a series of small molecules such as O_2, N_2, H_2, NO, and CO and we have found that relativistic density functional geometry optimizations and frequency calculations can greatly help the identification of these reaction products.[24−34]

* E-mail: lsa@virginia.edu; bursten.1@osu.edu.
† University of Virginia.
‡ The Ohio State University.

(1) Behr, A. *Carbon Dioxide Activation by Metal Complexes*; VCH: Weinheim, Germany, 1988. Solymosi, F. *J. Mol. Catal.* **1991**, *65*, 337.
(2) Creutz, C. in *Electrochemical and Electrocatalytic Reactions of Carbon Dioxide*; Sullivan, B. P., Krist, K., Guard, H. E., Eds.; Elsevier: Amsterdam, 1993.
(3) Gibson, D. H. *Chem. Rev.* **1996**, *96*, 2063.
(4) Leitner, W. *Coord. Chem. Rev.* **1996**, *153*, 257.
(5) Yin, X.; Moss, J. R. *Coord. Chem. Rev.* **1999**, *181*, 27.
(6) Huber, H.; Moskovits, M.; Ozin, G. A. *Nature Phys. Sci.* **1972**, *236*, 127.
(7) Mascetti, J.; Tranquille, M. *Surf. Sci.* **1985**, *156*, 20.
(8) Mascetti, J.; Tranquille, M. *J. Phys. Chem.* **1988**, *92*, 2173.
(9) Galan, G.; Fouassier, M.; Tranquille, M.; Mascetti, J.; Pàpai, I. *J. Phys. Chem. A* **1997**, *101*, 2626.
(10) Jeung, G. *Mol. Phys.* **1989**, *67*, 747.
(11) Caballol, R.; Sanchez Marcos, E.; Barthelat, J. C. *J. Phys. Chem.* **1987**, *91*, 1328.
(12) Sodupe, M.; Branchadell, V.; Oliva, A. *J. Phys. Chem.* **1995**, *99*, 8567.
(13) Sodupe, M.; Branchadell, V.; Rosi, M.; Bauschlicher, C. W., Jr. *J. Phys. Chem. A* **1997**, *101*, 7854.
(14) Pàpai, I.; Mascetti, J.; Fournier, R. *J. Phys. Chem. A* **1997**, *101*, 4465.
(15) Mascetti, J.; Galan, F.; Pàpai, I. *Coord. Chem. Rev.* **1999**, *190−192*, 557.
(16) Chertihin, G. V.; Andrews, L. *J. Am. Chem. Soc.* **1995**, *117*, 1595 (Ti + CO_2).
(17) Souter, P. F.; Andrews, L. *J. Chem. Soc., Chem. Commun.* **1997**, 777; *J. Am. Chem. Soc.* **1997**, *119*, 7350 (Cr, Mo, W + CO_2).
(18) Zhou, M. F.; Andrews, L. *J. Am. Chem. Soc.* **1998**, *120*, 13230 (Sc + CO_2).
(19) Zhou, M. F.; Andrews, L. *J. Phys. Chem. A* **1999**, *103*, 2013 (Cr − Cu + CO_2).
(20) Zhou, M. F.; Andrews, L. *J. Phys. Chem. A* **1999**, *103*, 2066 (V, Ti + CO_2).
(21) Wang, X. F.; Chen, M. H.; Zhang, L. N.; Qin, Q. Z. *J. Phys. Chem. A* **2000**, *104*, 758 (Ta + CO_2).
(22) Insertion reactions of CO_2 with organolanthanide complexes are known; see, for example: Evans, W. J.; Seibel, C. A.; Ziller, J. W.; Doedens, R. J. *Organometallics* **1998**, *17*, 2103 and references therein.
(23) Tague, T. J., Jr.; Andrews, L.; Hunt, R. D. *J. Phys. Chem.* **1993**, *97*, 10 920.
(24) Hunt, R. D.; Andrews, L *J. Chem. Phys.* **1993**, *98*, 3690.
(25) Zhou, M. F.; Andrews, L.; Ismail, N.; Marsden, C. *J. Phys. Chem. A* **2000**, *104*, 5495.
(26) Hunt, R. D.; Yustein, J. T.; Andrews, L. *J. Chem. Phys.* **1993**, *98*, 6070.
(27) Kushto, G. P.; Souter, P. F.; Andrews, L. *J. Chem. Phys.* **1998**, *108*, 7121.
(28) Souter, P. F.; Kushto, G. P.; Andrews, L.; Neurock, M. *J. Am. Chem. Soc.* **1997**, *119*, 1682.

10.1021/ja0016699 CCC: $19.00
Published on Web 11/05/2000

Table 1: Infrared Absorptions (cm^{-1}) from Laser-Ablated Uranium Atoms, Cations and Electrons Co-deposited with CO_2 in Excess Neon

$^{12}C^{16}O_2$	$^{13}C^{16}O_2$	$^{12}C^{18}O_2$	$^{12}CO_2 + {}^{13}CO_2$	$^{12}C^{16}O_2$ in Ar	identification
2374.8	2307.3		2374.8, 2307.3		$(U^+-OCO)^a$
2347.6	2281.8	2312.5	2347.6, 2281.8	2344.8	CO_2
2140.8	2093.7	2089.7	2140.8, 2093.7	2138.2	CO
2130.8	2074.5		2130.8, 2122.3, 2074.5		$C_2O_4^+$
2073.0	2027.6	2023.5	2073.2, 2027.6		$OUCO^+$
2045.0	1991.1	2033.9		2044.2	CO_3
2021.6	1976.7	1974.2	2021.6, 2003.4, 1976.7, 1956.8	2011.4	$O_2U(CO)_2$
2001	1957	1953			$O_2U(CO)_x$
1978.4	1936.6	1929.3	1978, 1936.6		inc on anneal, ?
1907.7	1864.5	1863.2	1907.7, 1864.5	1893.0	O_2UCO
1895.1	1832.6				CO_4^-
1868.4	1826.2	1823.3	1868.4, 1850.9, 1826.2	1864.1	$O_2U(CO)_2^-$
1852.4	1803.1	1825.7		1857.0	$C_2O_4^-$
1806.9	1767.8	1764.8	1806.9, 1767.8	1799.6	OUCO
1757.3	1718.1	1716.5	1757.3, 1734.1, 1718.1	1742.2	$O_2U(CO)_2^-$
1658.2	1614.0	1630.5	1658.2, 1614.0	1657.0	CO_2^-
1421.6	1380.2	1399.6	1421.6, 1380.2		CO_2^+
1274.4	1263.0	1227.5	1274.4, 1267.2, 1263.0		$C_2O_4^+$
1189.2	1181.4	1135.4		1184.8	$C_2O_4^-$
914.9	914.8	869 sh	914.6	775.7	UO_2
893.6	893.6	849.0	893.6	878.9	$O_2U(CO)_2$ site
889.0	889.0	844.9	889.0	874.1	$O_2U(CO)_2$
886.3	886.3	842.1	886	870.6	O_2UCO
881.2	881.2	834.1	881.2		$OUCO^+$
871.5	871.5	828.5	871.5		$O_2U(CO)_x$
823.2	823.2	779.4	823.2	804.2	OUCO
820.6	820.0	777.2	820.6	801.3	OUCO
769.1	769.1	728.1	769.0		photosensitive, ?

[a] Tentative assignment.

To explore the reactivity of CO_2 toward f-elements, we have carried out here a neon matrix infrared experimental and density functional theoretical investigation of the Th and U reaction with CO_2.

Experimental and Computational Section

The experiment for laser ablation and matrix isolation spectroscopy has been described in detail previously.[35,36] Briefly, the Nd:YAG laser fundamental (1064 nm, 10-Hz repetition rate with 10 ns pulse width) was focused on the rotating metal uranium or thorium target (Oak Ridge National Laboratory) using low energy (1−5 mJ/pulse) to minimize secondary processes. Laser-ablated metal atoms were co-deposited with carbon dioxide (0.05−0.2%) in excess neon onto a 4 K CsI cryogenic window at 2−4 mmol/h for 30 min to 1 h. Carbon dioxide (Matheson), $^{13}C^{16}O_2$ (Cambridge Isotopic Laboratories), a $^{12}CO_2 + {}^{13}CO_2$ mixture, and $C^{16}O^{18}O + C^{18}O_2$, 85% ^{18}O (Spectra Gases), were used in different experiments. Infrared spectra were recorded at 0.5-cm^{-1} resolution on a Nicolet 750 spectrometer with 0.1-cm^{-1} accuracy using a HgCdTe detector. Matrix samples were annealed at different temperatures, and selected samples were subjected to broad-band photolysis by a medium-pressure mercury arc (Philips, 175W, globe removed, $\lambda > 240$ nm). Additional experiments were done with CCl_4 added to the sample at 10% of CO_2 concentration to trap laser-ablated electrons and affect the product chemistry.[18−20,25]

Relativistic density functional theoretical (DFT) calculations have been performed by using the Amsterdam Density Functional (ADF 2.3) code,[37] with the inclusion of the generalized gradient approach of Perdew and Wang (PW91).[38] The [$1s^2$] cores for C and O and [$1s^2-5d^{10}$] core for Th and U were frozen via a frozen core approximation.[37a] Slater-type-orbital (STO) basis sets of triple-ζ quality were used for the valence orbitals of Th, U, C, and O, with d- and f-type polarization functions for the C and O. Numerical integration accuracy of INTEGRATION = 10.0 was used throughout.

The structures of calculated species were fully optimized with the inclusion of scalar (mass-velocity and Darwin) relativistic effects. When near-degenerate low-lying states were encountered, fractional occupation numbers were used to enforce the Aufbau principle. Vibrational frequencies were determined via numerical evaluation of the second-order derivatives of the total energies. As shown in our previous work,[39] good accuracy can be achieved when using the gradient-corrected PW91 functionals in frequency calculations of organoactinide systems. The atomic masses used in the frequency calculations for the isotopic substitution are 238.050 783 for ^{238}U, 12.000 00 and 13.003 35 for ^{12}C and ^{13}C, and 15.994 91 and 17.9992 for ^{16}O and ^{18}O, respectively.[40] Further computational details have been described elsewhere.[41]

Results

Infrared spectra of U and Th reaction products with CO_2 in excess neon and DFT calculations on anticipated product

(29) Souter, P. F.; Kushto, G. P.; Andrews, L.; Neurock, M. *J. Phys. Chem. A* **1997**, *101*, 1287.
(30) Kushto, G. P.; Souter, P. F.; Andrews, L.; Neurock, M. *J. Chem. Phys.* **1997**, *106*, 5894.
(31) Kushto, G. P.; Andrews, L. *J. Phys. Chem. A* **1999**, *103*, 4836.
(32) Zhou, M. F.; Andrews, L. *J. Chem. Phys.* **1999**, *111*, 4230.
(33) Zhou, M. F.; Andrews, L. Li, J.; Bursten, B. E. *J. Am. Chem. Soc.* **1999**, *121*, 9712 (U + CO).
(34) Zhou, M. F.; Andrews, L.; Li, J.; Bursten, B. E. *J. Am. Chem. Soc.* **1999**, *121*, 12 188. Li, J.; Bursten, B. E.; Zhou, M. F.; Andrews, L., to be published (Th + CO).
(35) Burkholder, T. R.; Andrews, L. *J. Chem. Phys.* **1991**, *95*, 8697.
(36) Hassanzadeh, P.; Andrews, L. *J. Phys. Chem.* **1992**, *96*, 9177.
(37) *ADF 2.3*, Theoretical Chemistry, Vrije Universiteit, Amsterdam: (a) Baerends, E. J.; Ellis, D. E.; Ros, P. *Chem. Phys.* **1973**, *2*, 42. (b) te Velde, G.; Baerends, E. J. *J. Comput. Phys.* **1992**, *99*, 94. (c) Fonseca Guerra, C.; Visser, O.; Snijders, J. G.; te Velde, G.; Baerends, E. J. In *Methods and Techniques for Computational Chemistry*; Clementi, E., Corongiu, G., Eds.; STEF: Cagliari, 1995; p 305.
(38) (a) Perdew, J. P.; Wang, Y. *Phys. Rev. B* **1992**, *45*, 13244. (b) Perdew, J. P.; Chevary, J. A.; Vosko, S. H.; Jackson, K. A.; Pederson, M. R.; Singh, D. J.; Foilhais, C. *Phys. Rev. B* **1992**, *46*, 6671.
(39) Li, J.; Bursten, B. E. *J. Am. Chem. Soc.* **1998**, *120*, 11456.
(40) Emsley, J. *The Elements*; Clarendon Press: Oxford, 1989.
(41) Li, J.; Bursten, B. E. *J. Am. Chem. Soc.* **1997**, *119*, 9021.
(42) Jacox, M. E.; Thompson, W. E. *J. Chem. Phys.* **1989**, *91*, 1410 (CO_2^+, CO_2^-).
(43) Jacox, M. E.; Thompson, W. E. *J. Phys. Chem.* **1991**, *95*, 2781 (CO_4^-).
(44) Zhou, M.; Andrews, L. *J. Chem. Phys.* **1999**, *110*, 2414 (CO_2^-, $C_2O_4^-$).
(45) Zhou, M.; Andrews, L. *J. Chem. Phys.* **1999**, *110*, 6820 ($C_2O_4^+$).

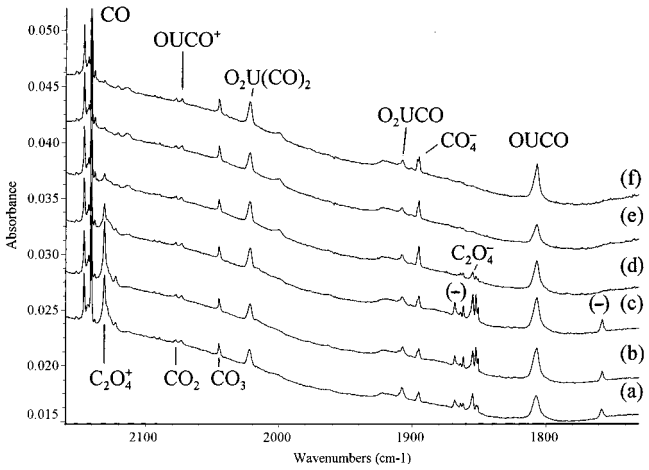

Figure 1. Infrared spectra in the 2160−1730-cm^{-1} region for laser-ablated U atoms, cations, and electrons co-deposited with 0.1% CO_2 in neon at 4 K. (a) 30-min sample co-deposition, (b) after 6 K annealing, (c) after $\lambda > 470$ nm photolysis, (d) after $\lambda > 290$ nm photolysis, (e) after $\lambda > 240$ nm photolysis, and (f) after annealing to 8 K.

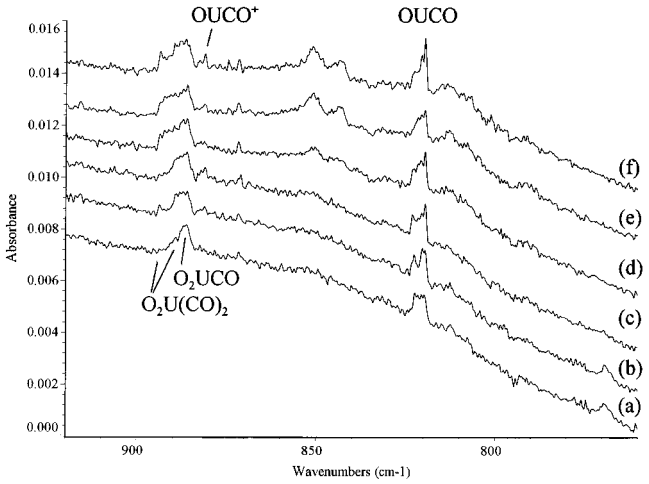

Figure 2. Infrared spectra in the 920−760 cm^{-1} region for laser-ablated U atoms, cations, and electrons co-deposited with 0.1% CO_2 in neon at 4 K. (a) 30-min sample co-deposition, (b) after 6 K annealing, (c) after $\lambda > 470$ nm photolysis, (d) after $\lambda > 290$ nm photolysis, (e) after $\lambda > 240$ nm photolysis, and (f) after annealing to 8 K.

molecules will be presented. The infrared spectra reveal a number of CO_2 related product bands common to U, Th, and other metal and neon discharge experiments. These bands[42−45] include CO, $C_2O_4^+$, CO_3, CO_4^-, $C_2O_4^-$, CO_2^-, and CO_2^+, and are listed in Table 1.

U and CO_2. The product spectrum in the carbonyl region for U and CO_2, Figure 1, is dominated by a new 1806.9-cm^{-1} band (OUCO) and, in the oxide region, Figure 2, reveals a split 823.2, 820.6 cm^{-1} absorption (OUCO). Note that these bands increase slightly on 6 K annealing, decrease slightly on $\lambda >$ 240 nm photolysis, and sharpen and increase on final 8 K annealing. Other new bands are observed in the carbonyl region: a 2021.6-cm^{-1} band increases slightly on annealing and a 1868.4, 1757.3 cm^{-1} pair (−) is destroyed by photolysis (with filters, $\lambda > 470$ nm increases both bands 40%, $\lambda > 380$ nm decreases both by 40%, and $\lambda > 290$ nm destroys both bands and markedly decreases CO_2^+, CO_2^-, $C_2O_4^+$ and $C_2O_4^-$ absorptions). Annealing slightly increases a new absorption at 2374.8 cm^{-1}, and in contrast, photolysis destroys the latter absorption and increases a new 2073.0-cm^{-1} band. The oxide region reveals new absorptions at 889.0 and 886.3 cm^{-1} on

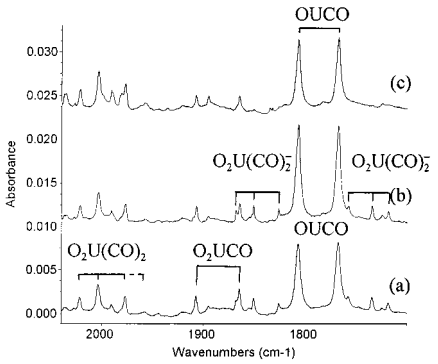

Figure 3. Infrared spectra in the 2040−1700-cm^{-1} region for laser-ablated U atoms, cations, and electrons co-deposited with 0.2% CO_2 in neon at 4 K. (a) 30 min co-deposition with 0.1% $^{12}CO_2$ + 0.1% $^{13}CO_2$, (b) after annealing to 6 K, and (c) after full-arc photolysis.

deposition, 893.6, 871.5 cm^{-1} on annealing, and 881.2 cm^{-1} on photolysis. The 769.1-cm^{-1} absorption is destroyed by photolysis (particularly $\lambda > 380$ nm).

One experiment was performed with CCl_4 added to serve as an electron trap using 0.2% CO_2 and 0.02% CCl_4: the effect of CCl_4 is to capture electrons, eliminate anions, and enhance cations. Here, as before,[44,45] CO_2^-, CO_4^-, and $C_2O_4^-$ were eliminated; the 2374.8-cm^{-1} band was increased, the relative 2073.0/1806.9-cm^{-1} band absorbance ratio was increased from $^1/_{10}$ to $^7/_{17}$ after photolysis, and the 1868.4-, 1757.3-cm^{-1} bands were eliminated (769.1-cm^{-1} was covered) by CCl_4.

Experiments were performed with $^{13}CO_2$ and $C^{18}O_2$, and the isotopic counterpart absorptions are listed in Table 1. An experiment with $^{12}CO_2$ + $^{13}CO_2$ (Figure 3) gave doublet absorptions for single carbonyl and triplet band patterns for dicarbonyl absorptions. The $C^{18}O_2$ sample contained sufficient $C^{16}O^{18}O$ to give $^{16}O^{18}O$ counterpart absorptions at 2070.1, 2002.6, 1838.7, 1806.9, 1733.1, 877.9, and 871.5 cm^{-1} for the $C^{18}O_2$ product bands at 2023.5, 1974.2, 1823.3, 1764.8, 1716.5, 849.0, and 844.9 cm^{-1}, respectively. The 823.2−779.4-cm^{-1} bands show no intermediate component.

Complementary argon matrix experiments were done at low laser energy to determine shifts and to increase product yield as CO_2 concentrations were increased to 0.5% and deposition to 1 h. Band positions are listed in Table 1. The major product bands (OUCO) are now observed at 1799.6 and 804.2 cm^{-1} (Figures 4 and 5) in agreement with previous work,[23] but only small amounts of UO and UO_2 are observed[24] at 819.6 and 775.7 cm^{-1}. Photolysis decreases sharp, weak 1864.1- and 1742.2-cm^{-1} features (−) and increases the 2011.4-cm^{-1} band; annealing to 35 K further increases the 2011.4-cm^{-1} band and associates an 874.1-cm^{-1} absorption ($O_2U(CO)_2$). The 1893.0- and 870.6-cm^{-1} bands (O_2UCO) increase slightly on photolysis and annealing. An experiment with 0.5% CO_2 and 0.05% CCl_4 gave all of the above bands except for the 1864.1, and 1742.2-cm^{-1} features. A $^{12}CO_2$ + $^{13}CO_2$ experiment revealed triplet absorptions at 2011.4, 1993.3, and 1966.8 cm^{-1} and doublet absorptions at 1893.0, 1850.6 cm^{-1} and at 1799.6, 1760.5 cm^{-1}. An experiment with the $C^{18}O_2$ sample gave major bands in the carbonyl region at 1964.1, 1849.6, and 1757.3 cm^{-1}, sharp, weak 1821.7- and 1701.6-cm^{-1} absorptions, and a $^{16}O^{18}O$ counterpart at 1992.5 cm^{-1} for the 2011.4−1964.1-cm^{-1} bands. In the oxide region, major bands were observed at 830.4, 827.2, and 761.6 cm^{-1}; the former showed clear 16−18 counterparts at 858.5 and 855.3 cm^{-1}, but the latter gave only the pure-16 counterpart as a weak band at 804.2 cm^{-1}.

Th and CO_2. Infrared spectra for the Th and CO_2 products in solid neon are illustrated in Figure 6, and the product

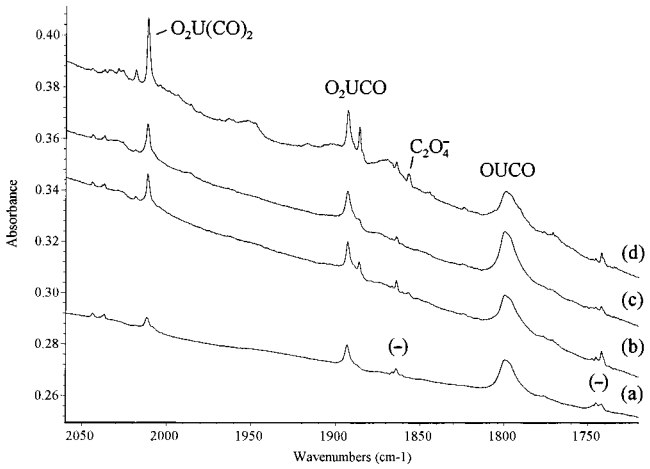

Figure 4. Infrared spectra in the 2160−1730-cm^{-1} region for laser-ablated U atoms, cations, and electrons co-deposited with 0.5% CO_2 in argon at 7 K. (a) 1-h sample co-deposition, (b) after 25 K annealing, (c) after $\lambda > 240$ nm photolysis, and (d) after 35 K annealing.

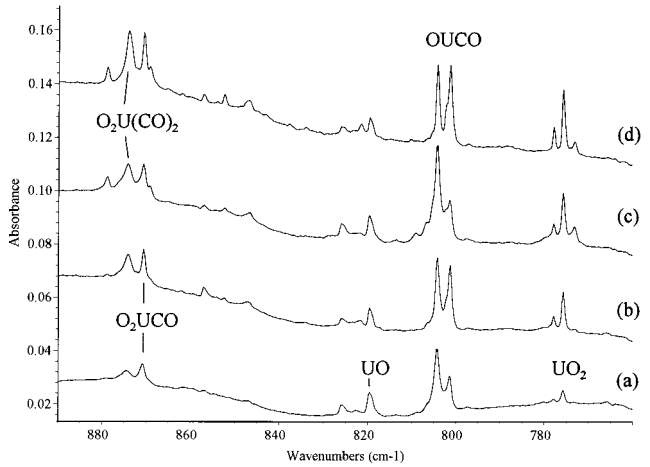

Figure 5. Infrared spectra in the 890−760-cm^{-1} region for laser-ablated U atoms, cations, and electrons co-deposited with 0.5% CO_2 in argon at 7 K. (a) 1-h sample co-deposition, (b) after 25 K annealing, (c) after $\lambda > 240$ nm photolysis, and (d) after 35 K annealing.

absorptions are listed in Table 2. The carbonyl region reveals major products at 2009.9 cm^{-1} ($OThCO^+$) and 1778.4 cm^{-1} (OThCO) and minor bands at 1951.5 and 1829.4 cm^{-1} (labeled (−)). In Figure 1, the 2009.9/1778.4 absorbance ratio is 8/9, but with 0.02% CCl_4 and 0.2% CO, this ratio increased to 17/5; a like increase was found for the 896.4/884.5 absorbance ratio. The 1951.5- and 1829.4-cm^{-1} bands were absent with CCl_4, but the 1976.3-cm^{-1} band was still observed. The oxide region contained 887.1- and 884.5-cm^{-1} bands for ThO, based on site splittings observed previously,[46] and a new band appeared at 896.4 cm^{-1}.

Again, experiments were done with $^{13}CO_2$ and $C^{18}O_2$. Mixed $^{12}CO_2 + {}^{13}CO_2$ gave doublet patterns for the 2009.9 and 1778.4 cm^{-1} bands, a triplet at 1951.5, 1932.4, 1908.3 cm^{-1}, but $^{13}C_2O_4^-$ obscured the region between the 1829.4- and 1788.6-cm^{-1} bands and the region below 1976.3 cm^{-1} was masked by other bands. The $C^{18}O_2 + C^{16}O^{18}O$ experiment gave $^{16}O^{18}O$ counterparts at 2009.9, 1931.0, 1774.0, and 884.5 cm^{-1} for the major $C^{18}O_2$ product bands at 1953.2, 1906.1, 1742.9, and 837.4 cm^{-1}.

Additional experiments employed argon matrix gas, and the band positions are listed in Table 2. The major absorptions were observed at 1965.6 and 1766.4 cm^{-1}, and these bands shifted

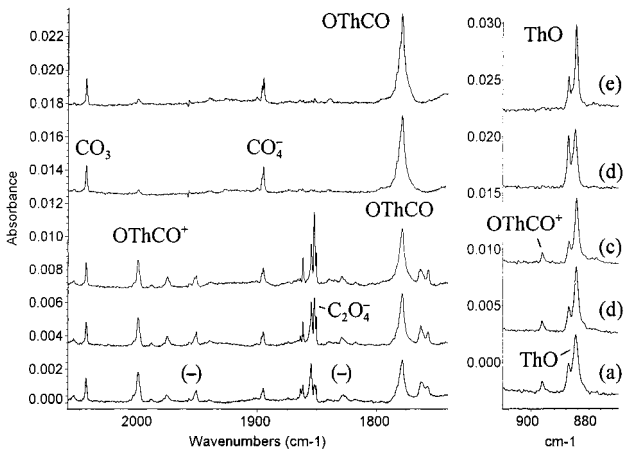

Figure 6. Infrared spectra in the 2060−1740- and 910−870-cm^{-1} regions for laser-ablated Th atoms, cations, and electrons co-deposited with 0.2% CO_2 in neon at 4 K. (a) 30-min sample co-deposition, (b) after 6 K annealing, (c) after 8 K annealing, (d) after full-arc photolysis, and (e) after 10 K annealing.

to 1918.4 and 1728.4 cm^{-1} with $C^{18}O_2$; the oxide region contained ThO at 878.8, 876.4 cm^{-1} and a new band at 829.8 cm^{-1} and $Th^{18}O$ at 831.9, 829.8 cm^{-1} and a new band at 785.7 cm^{-1} in these experiments.

Relativistic DFT Calculations. To assist in the identification and assignment of the new actinide product molecules, relativistic density functional calculations were performed. Generally several spin multiplicities and geometry structures were optimized to ferret out the most stable electronic states and geometries. Table 3 lists geometric parameters and stretching frequencies for the lowest energy structures found, and Figure 7 illustrates these structures.

We have optimized singlet, triplet, and quintet states of bent and linear structures for OUCO. For both linear and bent OUCO, the lowest energy state is a quintet, corresponding to four unpaired electrons. A lower energy is calculated for the $^5A''$ bent form of the molecule; although the linear $^5\Phi$ quintet is only 8.4 kcal/mol higher in energy, it has an imaginary degenerate bending frequency, consistent with it being a transition state between the two degenerate bent forms of the molecule. Interestingly, for the linear quintet, the calculated C−O stretching frequency is only 21 cm^{-1} lower and the U−O stretching frequency only 4 cm^{-1} higher than the values calculated for the optimized bent structure at 1842 and 859 cm^{-1}.

Similarly, geometry optimizations of the doublet, quartet, and sextet states of linear and bent $OUCO^+$ cation and $OUCO^-$ anion indicate that the quartet states are much more stable than the other low-spin or high-spin states, with the bent structure again more stable than the linear one. The frequency calculations indicate that the linear quartet states of $OUCO^+$ and $OUCO^-$ are only transition states with imaginary bending frequencies.

For the O_2UCO molecule, we have optimized singlet, triplet, and quintet states for two C_{2v} structures (T-shaped and umbrella-shaped) and two lower-symmetry C_s structures, where the CO was allowed to tilt in the two symmetry planes of the T-shaped structure. The triplets are lower in energy than the other spin states, and the $^3A_2$ state of the T-shaped O_2UCO molecule with C_{2v} symmetry has the lowest energy. The optimization of the C_s structure with the CO tilted out-of-UO_2-plane has given this T-shaped structure, which underscores the stability of the latter.

(46) Gabelnick, S. D.; Reedy, G. T.; Chasanov, M. G. *J. Chem. Phys.* **1974**, *60*, 1167 (ThO_2).

Table 2: Infrared Absorptions (cm^{-1}) from Laser-Ablated Thorium Atoms, Cations and Electrons Co-deposited with CO_2 in Excess Neon

$^{12}C^{16}O_2$	$^{13}C^{16}O_2$	$^{12}C^{18}O_2$	$^{12}CO_2 + {}^{13}CO_2$	$^{12}C^{16}O_2$ in Ar	identification
2140.8	2093.7	2089.7	2140.8, 2093.7	2138.2	CO
2009.9	1957.1	1953.2	2000.9, 1957.1	1965.6	$OThCO^+$
1976.3	1932.9	1929.2			$(O_2Th(CO)_2)$
1951.5	1908.3	1906.1	1951.5, 1932.4, 1908.3		$O_2Th(CO)_2^-$
1829.4	1788.6	1786.8	1829.4, ?, 1788.6		$O_2Th(CO)_2^-$
1778.4	1735.4	1742.9	1778.4, 1735.4	1766.4	OThCO
1762.8	1724.7	1720.5			OThCO site
1756.8	1718.9	1714.4		1742.2	OThCO site
896.4	896.4	848.6	896.4		$OThCO^+$
887.1	887.1	839.8	887.1	878.8	ThO
884.5	884.5	837.4	884.5	876.4	ThO
				829.8	OThCO
756.8	756.8	717.6	756.8		ThO_2, weak
739.6	739.6	701.2	739.6	722.1	ThO_2 complex
734.5	734.5	696.6	734.5	713.7	ThO_2 complex
726.2	726.2	688.5	726.2		ThO_2 complex

Table 3: Molecular Structures, Electronic States, Geometries, and Vibrational Frequencies and Intensities Calculated for Lowest Energy Uranium and Thorium Species[a]

molecule	structure	state	geometry	frequency and intensity
OUCO	bent (C_s)	$^5A''$	O−U = 1.828, U−C = 2.259, C−O = 1.174, ∠OUC = 113.8, ∠UCO = 179.1	1842 (942), 859 (236), 325 (1), 274 (5)
$OUCO^-$	bent (C_s)	$^4A'$	O−U = 1.848, U−C = 2.272, C−O = 1.192, ∠OUC = 109.6, ∠UCO = 179.4	1744 (1155), 810 (221), 507 (1), 306 (1)
$OUCO^+$	bent (C_s)	$^4A''$	O−U = 1.795, U−C = 2.323, C−O = 1.152, ∠OUC = 103.9, ∠UCO = 178.2	2007 (630), 915 (195)
O_2UCO	T-shaped (C_{2v})	$^3A_2$	O−U = 1.818, U−C = 2.305, C−O = 1.172, ∠OUO = 163.1, ∠UCO = 180.0	1866 (1123), 874 (390), 803(51)
$OU(CO)_2$	bent (C_s)	$^3A''$	O−U = 1.821, U−C = 2.205, C−O = 1.177, ∠OUCC = 97.1, ∠CUC = 64.7, ∠UCO = 178.5	1851 (890), 1777 (773), 865 (214), 485 (16)
$O_2U(CO)_2$	tetrahedral (C_{2v})	$^1A_1$	O−U = 1.806, U−C = 2.294, C−O = 1.162, ∠OUO = 177.8, ∠CUC = 65.1, ∠UCO = 177.5	1975 (416), 1893 (797), 908 (366), 828 (38)
$O_2U(CO)_2^-$	tetrahedral (C_{2v})	$^2A_2$	O−U = 1.852, U−C = 2.254, C−O = 1.187, ∠OUO = 161.4, ∠CUC = 71.7, ∠UCO = 179.6	1808 (914), 1708 (1419), 811 (428), 751 (83)
$O_2U(CO)_2^-$	tetrahedral (C_{2v})	$^4B_1$	O−U = 1.856, U−C = 2.344, C−O = 1.186, ∠OUO = 152.9, ∠CUC = 106.5, ∠UCO = 179.1	1811 (400), 1748 (2133), 807 (421), 755 (123)[b]
ThO	linear ($C_{\infty v}$)	$^1\Sigma^+$	O−Th = 1.853	882 (175)
ThO_2	bent (C_{2v})	$^1A_1$	O−Th = 1.911, ∠OThO = 114.2	812 (103), 759 (291), 157 (52)
OThCO	bent (C_s)	$^3A''$	O−Th = 1.871, Th−C = 2.488, C−O = 1.161, ∠OThC = 90.8, ∠ThCO = 176.8	1789 (2089), 850 (197)
$OThCO^-$	bent (C_s)	$^4A''$	O−Th = 1.917, Th−C = 2.392, C−O = 1.202, ∠OThC = 108.1, ∠ThCO = 166.0	1667 (1251), 785 (214)
$OThCO^+$	bent (C_s)	$^2A''$	O−Th = 1.838, Th−C = 2.465, C−O = 1.147, ∠OThC = 92.5, ∠ThCO = 176.5	1993 (498), 914 (141)
$O_2Th(CO)_2^-$	tetrahedral (C_{2v})	$^2A_1$	O−Th = 1.967, Th−C = 2.623, C−O = 1.167, ∠OThO = 133.0, ∠CThC = 72.1, ∠ThCO = 179.5	1919 (938), 1830 (1848), 704 (166), 680 (372)
$O_2Th(CO)_2^{2-}$	tetrahedral (C_{2v})	$^1A_1$	O−Th = 2.017, Th−C = 2.548, C−O = 1.195, ∠OThO = 129.3, ∠CThC = 54.5, ∠ThCO = 174.2	1725 (2340), 1686 (652), 648 (103), 616 (418)

[a] The bond lengths in Å, angles in deg, frequencies in cm^{-1}, and intensities (in parentheses) in km/mol. [b] The $^4B_1$ quartet is only 6.1 kcal/mol above the doublet.

Singlet, triplet, and quintet structures of $O_2U(CO)_2$ have been optimized in planar (C_{2v} and D_{2h}), pseudotetrahedral (C_{2v}), and low symmetry (C_2) structures. Optimization of the C_2 symmetry structures lead to pseudotetrahedral geometries, and the stabilities of different structures decrease as pseudotetrahedral > planar D_{2h} > planar C_{2v}. The $^1A_1$ singlet pseudotetrahedral structure has the lowest energy, and the planar D_{2h} structure (the transition state between two degenerate pseudotetrahedral structures) is 13.7 kcal/mol higher in energy. However, there exist three low-lying triplet states, $^3A_2$ (3.6 kcal/mol higher), $^3B_1$ (6.9 kcal/mol), and $^3B_2$ (7.3 kcal/mol), which will contribute to the ground state when taking account of spin−orbit coupling effects. The $O_2U(CO)_2^-$ anion has a $^2A_2$ doublet with the same minimum energy geometry, although a $^4B_1$ quartet state lies only 6.1 kcal/mol higher in energy.

For the thorium-containing molecules, we first calculated the states and geometries of ThO and ThO_2 as test cases. The lowest state of ThO is a singlet ($^1\Sigma^+$) with Th−O = 1.853 Å and ν = 882 cm^{-1} (175 km/mol intensity). This calculated frequency compares favorably to that observed for ThO in solid neon,[34] 887.1 cm^{-1}. The singlet state of ThO corresponds to a $7s^25f^06d^0$ configuration for the Th(II) center. ThO_2 is found to be a bent singlet ($^1A_1$) molecule with ∠O−Th−O = 114.2°, Th−O = 1.911 Å and frequencies 157 (52 km/mol), 759 (291), 812 cm^{-1} (103). The latter two frequencies are very close to the 756.8 and 808.4 cm^{-1} antisymmetric and symmetric stretching fundamentals observed by us in a neon matrix, and the calculated angle is comparable to the experimentally determined value of 122.5°(±2°) as based on the matrix IR spectral isotopic shifts.[46] These results on ThO_2 are very similar to those obtained in a previous DFT (B3LYP) calculation of the molecule, which found geometric parameters of 118.8° and 1.906 Å and frequencies of 159, 760, 802 cm^{-1}.[47]

We have calculated the lowest-energy singlet, triplet, and quintet states of linear and bent OThCO structures. In both the

(47) Zhou, M. F.; Andrews, L. *J. Chem. Phys.* **1999**, *111*, 11044.

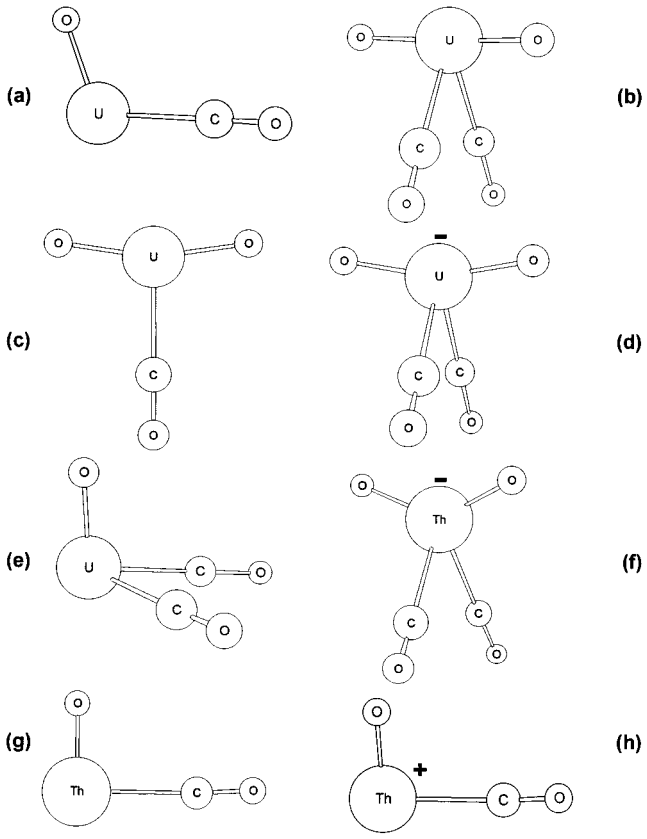

Figure 7. Molecular structures of (a) OUCO, (b) $O_2U(CO)_2$, (c) O_2-UCO, (d) $O_2U(CO)_2^-$, (e) $OU(CO)_2$, (f) $O_2Th(CO)_2^-$, (g) OThCO, and (h) $OThCO^+$. For geometry parameters, see Table 3.

linear and bent geometries, the triplet states are lowest in energy, with the bent form lower than the linear form. The calculated CO-stretching frequency in OThCO, 1789 cm^{-1}, is lower than the corresponding calculated frequency in OUCO, 1842 cm^{-1}, which agrees with the experimental observation. In addition, the calculations also reveal that $OThCO^+$ and $OThCO^-$ ions also prefer bent structures, with $^2A''$ and $^4A''$ ground states, respectively.

For the $O_2Th(CO)_2^-$ anion we have optimized the doublet, quartet, and sextet states with planar (C_{2v} and C_s), pseudotetrahedral (C_{2v}), and a low-symmetry (C_2) geometries. The ground state is a $^2A_1$ state with pseudotetrahedral geometry. While the planar C_{2v} structure is higher in energy, optimizations of all the C_2 and C_s structures have lead to the most stable pseudotetrahedral geometry. We will discuss the vibrational properties of these molecules in the following section.

Discussion

The new actinide product absorptions will be assigned on the basis of isotopic shifts, comparison between neon and argon matrix spectra, and relativistic DFT frequency calculations.

OUCO. The major absorptions at 1806.9 and 823.2 cm^{-1} in the uranium experiments are assigned to the uranium atom−CO_2-insertion product OUCO. The low laser energies employed here generate a relatively low metal atom concentration, much less than the CO_2 reagent, and the reactions are dominated by single metal atom processes. Relativistic DFT calculations predict strong stretching modes for bent $^5A''$ quintet OUCO at 1842- and 859-cm^{-1}, just 1.9 and 4.4% higher than the observed values. In addition, the theoretical vibrational displacements identify the 1842 and 859 cm^{-1} bands as C−O and U−O stretching vibrations. The $^{12}CO_2/^{13}CO_2$ (hereafter 12/13) and $C^{16}O_2/C^{18}O_2$ (hereafter 16/18) isotopic frequency ratios, 1.0221 and 1.0239, are appropriate for a C−O stretching mode (1.0225 and 1.0244 for CO), and the 16/18 ratio for the 823.2-cm^{-1} band (1.0562) matches that for UO (1.0564). The calculated 12/13 and 16/18 isotopic frequency ratios are 1.0229 and 1.0243 for the C−O stretching mode, and the 16/18 ratio is 1.0565 for the U−O stretching mode, in excellent agreement with these experimental ratios. Furthermore, mixed isotopic experiments ($^{12}CO_2 + {}^{13}CO_2$ and $C^{16}O^{18}O + C^{18}O_2$) give doublets in both regions and verify that only one CO submolecule and one UO subunit are involved in the observed vibrations. The near match of the isotopic frequency ratios to those of the diatomic models CO and UO implies that there is essentially no coupling between the C−O and U−O vibrations of OUCO, which is also indicated by the vibrational normal-mode analysis.

Because of the stronger matrix interaction for Ar than for Ne,[48] the 1799.6- and 804.4-cm^{-1} argon matrix bands[23] for OUCO are red shifted from the 1806.9 and 823.2-cm^{-1} neon matrix counterparts, which is reasonable for such a molecule as OUCO. The U−O absorption is split in both matrix hosts but the C−O band is not. The small neon−argon shift confirms that the same $^5A''$ OUCO electronic state is trapped in solid neon and argon, which is in contrast to the similar CUO molecule, where different states (singlet and triplet) are trapped in solid neon and argon, respectively.[33,49]

$OUCO^+$. The weak band at 2073.0 cm^{-1} increases slightly during the photolysis sequence illustrated in Figure 1 and sharpens on 8 K annealing. In experiments where $\lambda > 240$ nm photolysis was performed after 8 K annealing, the 2073.0-cm^{-1} band doubled, while the 1806.9-cm^{-1} OUCO band decreased by 20%. The 2073.0 cm^{-1} band shifts to 2027.6 cm^{-1} with $^{13}CO_2$ and to 2023.9 cm^{-1} with $C^{18}O_2$; the isotopic frequency ratios, 1.0224 and 1.0245, are appropriate for a C−O stretching mode. The $^{12}CO_2 + {}^{13}CO_2$ experiment gave a 2073.0−2027.6-cm^{-1} doublet, which shows that one CO molecule is involved; the $C^{16}O^{18}O + C^{18}O_2$ sample produced a 2070.1−2023.5-cm^{-1} doublet, which also shows that one CO molecule is involved but that coupling exists between the subunits as the $^{16}X-C^{16}O$ product (2073.0 cm^{-1}) is slightly different from the $^{18}X-C^{16}O$ product (2070.1 cm^{-1}). This coupling is a consequence of mode mixing, which is different in $OUCO^+$ and OUCO. A weak 881.2-cm^{-1} band is associated with the 2073.0-cm^{-1} band on annealing and photolysis. When $^{12}C^{18}O_2$ is used, this band shifts to 834.1 cm^{-1} (ratio 1.0565), which is the ratio expected for a U−O vibration. Hence, the absorber responsible for the 2073.0- and 881.2-cm^{-1} bands appears to contain CO and UO subunits.

Critical diagnostic information is found in the CCl_4-doped sample: the marked enhancement of the 2073.0- and 881.2-cm^{-1} bands relative to the 1806.9- and 823.2-cm^{-1} OUCO absorptions strongly supports identification of the 2073.0- and 881.2-cm^{-1} absorber as a cation.[18−20,25] All of the above information supports assignment of these bands to $OUCO^+$. The bands of this cation are 266.1 and 58.0 cm^{-1}, respectively, higher than the corresponding 1806.9- and 823.2-cm^{-1} bands for OUCO. Finally, the $OUCO^+$ cation was observed in neon but not argon as the more inert matrix is a better host for trapping cations.[42−45]

Our DFT calculations find a bent $^4A''$ quartet structure for $OUCO^+$ with calculated C−O and U−O stretching frequencies of 2007 and 915 cm^{-1}. The former is 3.2% lower than observed and the latter is 3.8% higher, which are comparable to the above agreement between calculated and observed frequencies for

(48) Jacox, M. E. *Chem. Phys.* **1994**, *189*, 149.
(49) Andrews, L.; Liang, B.; Li, J.; Bursten, B. E. *Angew Chem. Int. Ed.* **2000**, *39*, in press.

OUCO. The linear quartet U^+-OCO complex is calculated to be 3.5 eV higher in energy than $OUCO^+$, and to have a very strong OCO mode at 2375 cm^{-1}.

(U^+-OCO) Complex. The photosensitive 2374.8-cm^{-1} band shifts to 2307.3 cm^{-1} with $^{13}CO_2$ and exhibits almost the same 12/13 ratio as CO_2 itself. This band is clearly due to a perturbed CO_2 mode and the blue shift suggests the electrostatic interaction of a cation. Doping with CCl_4 produced a 5-fold increase in the 2374.8-cm^{-1} band relative to OUCO, and a cation complex is confirmed. The 2374.8 cm^{-1} band is tentatively assigned to the linear U^+-OCO complex trapped in the neon matrix.

OThCO. The strongest absorption at 1778.4 cm^{-1} in the thorium experiments is assigned to the OThCO insertion product. Our relativistic DFT calculations find the bent $^3A''$ triplet lowest energy structure with 1789 cm^{-1} (2089 km/mol) and much weaker 850 cm^{-1} (197 km/mol) stretching frequencies; the former is 0.6% higher than the observed value and the latter is too weak to be observed here. The 12/13 and 16/18 isotopic frequency ratios, 1.0248 and 1.0204, are unusual for a carbonyl stretching mode. The 12/13 ratio is high and the 16/18 ratio is low, even more so than for OWCO and OTaCO,[17,21] where metal−carbon bonding increases the carbon participation, even more than in heavy metal carbonyls such as HfCO.[50] The mixed isotopic experiments show no intermediate components for either neon and argon matrix band and confirm that single CO and ThO submolecules are involved in this molecule. The experiment with $C^{18}O_2$ and $C^{16}O^{18}O$ gave a 1774.0-cm^{-1} band for the $^{18}OThC^{16}O$ molecule, which confirms that a single CO_2 molecule is involved.

$OThCO^+$. In like fashion the 2000.9- and 896.4-cm^{-1} bands are assigned to $OThCO^+$. Similar calculations predict 1993- and 914-cm^{-1} stretching modes, just 0.4% lower and 2.0% higher than observed for bent doublet $OThCO^+$. The 12/13 and 16/18 isotopic frequency ratios 1.0224 and 1.0244 for the upper band are nearly that for CO and the 16/18 ratio 1.0563 for the lower band is essentially the same as ThO. These bands exhibit doublets in both mixed isotopic experiments so single CO and ThO subunits participate in these modes. The bands are nearly destroyed by broadband photolysis and markedly enhanced on the addition of CCl_4, which captures electrons and enhances the yield of metal cation reaction products.[18−20,24] Furthermore, the argon matrix counterpart of the upper band at 1965.6 cm^{-1} shows a much larger red shift from the neon value (35.3 cm^{-1}) than the corresponding OThCO band (12.0 cm^{-1}) as expected for a cation compared to a neutral molecule.

O_2UCO. The 1907.7-cm^{-1} band decreases and sharpens on annealing. The 12/13 and 16/18 ratios, 1.0232 and 1.0239, respectively, show more carbon and less oxygen motion than a typical carbonyl. The $^{12}CO + ^{13}CO$ experiment reveals a doublet for a monocarbonyl species. Since UCO has been reported at 1917.8 cm^{-1} and OUCO here at 1806.9 cm^{-1}, the next most likely monocarbonyl is O_2UCO.

Our DFT calculations predict frequencies of 1877 (640), 868 (380), and 871 cm^{-1} (117 km/mol) for the $^3A_2$ ground-state O_2UCO molecule and 12/13 and 16/18 ratios 1.0232 and 1.0242 for the carbonyl mode. Agreement with the 1907.7-cm^{-1} band and the observed isotopic frequency ratios is excellent. It is likely that the 886.3-cm^{-1} absorption, which decreases on annealing, is due to O_2UCO, but we cannot be certain. These bands are compatible with argon matrix absorptions at 1893.4 and 871.0 cm^{-1} assigned previously to O_2UCO,[23] and the present 1893.0, 870.6 cm^{-1} observations.

$O_2U(CO)_2$. The 2021.6-cm^{-1} band is the second strongest uranium product absorption; it shifts to 1976.7 cm^{-1} with $^{13}CO_2$ and to 1974.2 cm^{-1} with $C^{18}O_2$ (ratios 1.0227 and 1.0240), which is appropriate for a carbonyl mode. This band forms an asymmetric triplet (Figure 3) at 2021.6, 2003.4, 1976.7 cm^{-1} with $^{12}CO_2 + ^{13}CO_2$ and a new mixed isotopic band at 1956.8 cm^{-1} appears to be associated with this multiplet. Clearly, a dicarbonyl mode is involved here. In the $C^{18}O_2$ experiment, the major band shifts to 1974.2 cm^{-1} and an intermediate 2002.6-cm^{-1} absorption was observed for the carbonyl product with one ^{16}O and one ^{18}O atom providing more evidence for a dicarbonyl. The 2021.6-cm^{-1} band increases about 50% on annealing, while the 1907.7-cm^{-1} O_2UCO band and CO decrease a like amount so the $O_2U(CO)_2$ assignment for the 2021.6 band is a strong possibility. The 889.0-cm^{-1} band tracks with the 2021.6-cm^{-1} absorption on annealing. This band shifts to 844.9 cm^{-1} with $C^{18}O_2$ and gives the 1.0522 isotopic 16/18 frequency ratio appropriate for a UO_2 fundamental.[23,24] The intermediate 871.5-cm^{-1} band with $C^{16}O^{18}O$ verifies that two equivalent O atoms contribute to this vibration, which is due to a UO_2 moiety. Argon matrix counterparts at 2011.4 and 874.1 cm^{-1} are shifted as expected for the matrix hosts.[48]

Our DFT calculations predict a singlet ground state for $O_2U(CO)_2$, which is essentially linear OUO (177.8°) with two equatorial CO groups at an acute C−U−C angle of 65°. The closed-shell $(10a_1)^2(3a_2)^0$ configuration of $O_2U(CO)_2$ singlet is somewhat surprising because the neutral UO_2 molecule prefers a triplet with $(7s)^1(5f)^1$ configuration. Bonding analysis shows that the back-bonding of U 6d (12%) and 5f (38%) to the in-plane pπ orbitals of CO (25%C + 20% O) gives rise to the stabilization of the HOMO ($10a_1$), which favors a closed-shell electronic structure. However, the existence of three low-lying charge-transfer triplet states, especially the $^3A_2$ triplet, will greatly complicate the calculations of ground-state properties because all these three triplets will have a A_1 double-group component when spin−orbit coupling is taken into account. The $^3A_2$ triplet is only 3.6 kcal/mol higher than the $^1A_1$ singlet and has a $(10a_1)^1(3a_2)^1$ configuration, where the $3a_2$ orbital is composed of 76%f_{zxy} and 14%C + 7%O in the CO.

The calculated singlet antisymmetric O−U−O stretch has a frequency of 908 cm^{-1}, which is 19 cm^{-1} (2.1%) higher than the observed band frequency. The $U(CO)_2$ fragment of this molecule is reminiscent of the isolated $U(CO)_2$ molecule, which has a calculated C−U−C angle of 76°. This unusual acute angle is consistent with the unusual 5:1 symmetric:antisymmetric intensity ratio observed experimentally for the $U(CO)_2$ molecule.[33] In the case of $O_2U(CO)_2$, the intercarbonyl angle is even more acute than that in $U(CO)_2$, which should lead to an even greater symmetric:antisymmetric intensity ratio. We believe that the 2021.6-cm^{-1} band is due to the symmetric stretch of the CO ligands. The corresponding antisymmetric stretching mode, which is expected to be much weaker, is not observed except in the lower symmetry $O_2U(^{12}CO)(^{13}CO)$ molecule, which appears to have a band at 1956.8 cm^{-1}. If this latter band is assigned correctly, we can estimate that the antisymmetric C−O stretch in $O_2U(^{12}CO)_2$ would occur at ca. 1980 cm^{-1}. Our DFT calculation predicts the symmetric C−O mode at 1975 cm^{-1} (2.3% low). However, the antisymmetric mode is calculated to occur at 1893 cm^{-1} and with greater intensity than the symmetric stretch. Both of these calculated quantities appear to be in error; the frequency seems too low based on the observation of the 1956.8 cm^{-1} band in the mixed isotopomer, and the calculated intensity ratio is clearly inconsistent with the calculated acute

(50) Zhou, M. F.; Andrews, L. *J. Am. Chem. Soc.* **2000**, *122*, 1531.

C−U−C angle.[51] We have previously observed these difficulties in calculating intensities of the CO-stretching modes in acutely angled actinide dicarbonyls, such as $U(CO)_2$.[33] We have also seen the reverse problem in $Hf(CO)_2$, which has a C−Hf−C angle of 96.6° ($^3B_2$) or 132.5° ($^1A_1$, 2.5 kcal/mol higher). In that molecule, the symmetric stretch is calculated to be more intense than the antisymmetric stretch, which is inconsistent with the obtuse intercarbonyl angle.[50] These difficulties in calculating the intensities of the CO-stretching modes in dicarbonyls are vexing and warrant further investigation. Inasmuch as the singlet and triplet separations in the $O_2U(CO)_2$, $U(CO)_2$, and $Hf(CO)_2$ are quite small, state-mixing due to spin−orbit coupling effects will play a central role in determining the molecular geometry and the vibrational intensities of these molecules. Despite the problems with the calculated intensities of the carbonyl modes, the 12/13 and 16/18 isotopic frequency ratios are calculated to be 1.0233 and 1.0238 for the 1975-cm^{-1} band, and the 16/18 ratio is 1.0521 for the 908-cm^{-1} band, in reasonable agreement with the above experimental ratios. We therefore conclude that the 2021.6- and 889.0-cm^{-1} bands are probably due to the $O_2U(CO)_2$ molecule. Analogous $O_2M(CO)_2$ molecules have been detected for the third-row transition metals Ta and W. The CO-stretching frequencies in $O_2Ta(CO)_2$ (2126, 2016 cm^{-1})[21] and $O_2W(CO)_2$ (2091, 1998 cm^{-1})[17] are higher than those in $O_2U(CO)_2$ (2021, 1980 cm^{-1}, estimated from $O_2U(^{12}CO)(^{13}CO)$), which might indicate more significant metal−ligand back-bonding in the U complex.

$O_2U(CO)_2^-$. The 1868.4- and 1757.3-cm^{-1} bands increase together on 8 K annealing and on $\lambda > 470$ nm photolysis before decreasing on $\lambda > 380$ nm irradiation and disappearing on ultraviolet photolysis. The bands are eliminated by CCl_4 doping, which suggests a molecular anion.[18−20,25,44] Both bands reveal triplet absorptions with $^{12}CO + {}^{13}CO$ indicating the vibration of two equivalent carbonyl subunits and appropriate $C^{18}O_2$ shifts for a carbonyl vibration. Argon matrix counterparts were observed slightly shifted to 1864.1 and 1742.2 cm^{-1}.

The $^2A_2$ doublet state of $O_2U(CO)_2^-$ anion ($\angle CUC = 71.7°$) was calculated by DFT and 1808 cm^{-1} (914 km/mol) and 1708 (1419) symmetric and antisymmetric C−O frequencies were found. The $^4B_1$ quartet ($\angle CUC = 106.5°$), only 6.1 kcal/mol higher in energy, has the symmetric and antisymmetric C−O frequencies as 1811 (921) and 1748 cm^{-1} (2133 km/mol). Spin−orbit coupling will once again mix these two states because of their energy closeness. The strongest mode of $O_2Ta(CO)_2^-$ has been observed at 1838.8 cm^{-1}, which is 81.5 cm^{-1} higher than the corresponding value for uranium.

$O_2Th(CO)_2$. The weak 1976.3-cm^{-1} band increases on 6 and 8 K annealing and is destroyed on full-arc photolysis. The $^{13}CO_2$ and $C^{18}O_2$ counterparts give the 1.0225 and 1.0244 ratios characteristic of a C−O vibrational mode. Unfortunately, the region was congested and no mixed isotopic components could be observed. This weak band is tentatively assigned to $O_2Th(CO)_2$ following the example of uranium. The thorium analogue is much less stable and probably expels CO on photolysis leading to the increase observed in the 726.2-cm^{-1} ThO_2 complex absorption system.

$O_2Th(CO)_2^-$. Weak bands at 1951.5 and 1829.4 cm^{-1} in thorium experiments, were also destroyed by photolysis and eliminated by CCl_4 doping.[18−20,25,44] The 1951.5-cm^{-1} band gave a triplet absorption with $^{12}CO + {}^{13}CO$ and an intermediate component with $C^{16}O^{18}O$, but the middle region for the 1829.4-cm^{-1} band was masked so a possible triplet could not be observed.

Our DFT calculations for $O_2Th(CO)_2^-$ predicted the C−O symmetric and antisymmetric stretching frequencies and intensities at 1919 cm^{-1} (938 km/mol) and 1830 cm^{-1} (1848 km/mol), respectively. The symmetric and antisymmetric ThO_2 subunit stretching frequencies are calculated at 704 cm^{-1} (166 km/mol) and 680 cm^{-1} (371 km/mol). While these calculated frequencies for $O_2Th(CO)_2^-$ anion are in good agreement with the observed values, the frequencies determined for $O_2Th(CO)_2^{2-}$ dianion, 1725 cm^{-1} (2341 km/mol) and 1686 cm^{-1} (652) km/mol, are much lower compared to the above experimental data. These theoretical results support the assignment of $O_2Th(CO)_2^-$ anion. Note that the $O_2U(CO)_2^-$ frequencies are 83 and 72 cm^{-1} lower than the $O_2Th(CO)_2^-$ values, which is consistent with greater back-bonding in the U anion. This again underscores the fact that uranium has more electrons than thorium, as has been noted in a comparison of the bonding in CThO and CUO.[34] Since ThO_2 has a stable closed-shell, it is interesting to see where the extra electron goes in the dicarbonyl complex anion $O_2Th(CO)_2^-$. The Mulliken population analysis indicates that the spin densities are mainly distributed in the C (61%) and O (16%) atoms of the two CO ligands, with little at Th atom (23%). In contrast, the spin densities are 87% for U and 22% for CO (16% C + 6% O) in the $O_2U(CO)_2^-$ anion. One can therefore conclude that Th still prefers Th(IV) instead of Th(III) even in an anion.

Reaction Mechanisms. The major reaction during condensation of uranium and thorium atoms with CO_2 in excess neon is the spontaneous insertion reaction of the actinide metal atoms, which proceeds even on annealing the 4 K neon matrix to 6 K (Figures 1 and 6). The observation of complementary $^{18}OAnC^{16}O$ and $^{16}OAnC^{18}O$ absorptions in the $C^{16}O^{18}O$ experiment confirms that a single CO_2 molecule is involved in the insertion reaction 1. The secondary reaction with another CO_2 molecule to form the dioxo dicarbonyl also appears to be spontaneous, reaction 2a. These products can attach an electron to form the corresponding anions, reaction 3. For uranium, reaction 2a is exothermic by 46 kcal/mol. Another secondary product is also formed with uranium, reaction 2b, which is exothermic by 51 kcal/mol; however, the related secondary product $OU(CO)_2$ + O atom is higher in energy (by 164 kcal/mol) than O_2UCO + CO, and as a result $OU(CO)_2$ is not observed here.

$$An + CO_2 \rightarrow OAnCO \ (An = Th, U) \quad (1)$$

$$OAnCO + CO_2 \rightarrow O_2An(CO)_2 \quad (2a)$$

$$OUCO + CO_2 \rightarrow O_2UCO + CO \quad (2b)$$

$$O_2An(CO)_2 + e^- \rightarrow O_2An(CO)_2^- \quad (3)$$

The $O_2An(CO)_2^-$ anion is also stable as this is the major anion product for both actinide metals. The calculated electron affinity for $O_2U(CO)_2^-$ (1.5 eV) shows that this is a stable anion although it is decreased by $\lambda > 380$ nm photolysis (3.3 eV) and destroyed by $\lambda > 290$ nm radiation (4.3 eV), which in the case of uranium gave a 20% increase in the $O_2U(CO)_2$ absorption, reaction 4. The $O_2An(CO)_2^-$ anion products were absent with CCl_4 doping as CCl_4 preferentially captures the laser-ablated electrons[18−20,25,44] before $O_2An(CO)_2$ has the opportunity.

$$O_2U(CO)_2^- \xrightarrow{\lambda > 290 \text{ nm}} O_2U(CO)_2 + e^- \quad (4)$$

The actinide cations also insert into CO_2 and reaction 5 is probably spontaneous as the $OUCO^+$ absorptions increase

(51) The low-lying $^3A_2$ triplet has a larger ∠CUC angle (75.5°) and a short C−O bond length (1.156 Å) than those (65.1° and 1.162 Å) in the singlet, which will help to increase the C−O frequency and decrease the intensity of antisymmetric C−O stretching mode when spin−orbit coupling is included.

slightly on annealing the 4 K neon matrix to 6 and 8 K. The

$$An^+ + CO_2 \rightarrow OAnCO^+ \ (An = Th, U) \qquad (5)$$

overall yield of $OThCO^+$ is higher than that of $OUCO^+$ in these experiments although $OUCO^+$ absorptions increase by 50% on $\lambda > 240$ nm photolysis, whereas $OThCO^+$ is destroyed and OThCO increases. The yield of both $OAnCO^+$ cations is increased on doping with CCl_4 as the ablated electrons are captured by CCl_4 that would normally be fated to neutralize some of the cations.[18−20,25] It is possible for $\lambda > 240$ nm radiation (5.2 eV) to photoionize OUCO in the matrix cage as the computed ionization energy is 6.2 eV and a matrix shift on the order of 1 eV in the ionization energy is reasonable.[52] The $OThCO^+$ cation can also be produced in the same way, as the computed ionization energy is 6.0 eV, but this cation may be neutralized by photodetachment from anions in the system. It is also possible that a U^+-OCO complex rearranges to the more stable $OUCO^+$ on photolysis.

Although reaction 5 clearly contributes to the $OAnCO^+$ yield, direct photoionization by the laser plume on the target surface also produces the $OAnCO^+$ cations during matrix formation. The latter photoionization mechanism accounts for the formation of CO_2^+ and $(CO_2)_2^+$ in these neon matrix experiments.[45]

Finally, the amount of free CO in these experiments is just above the background level for a laser-ablation experiment and probably arises from CO_2 precursor photodissociation. The amount of CO present is insufficient for detection of reaction products.[33,34]

Bonding in OAnCO Complexes. The actinide oxocarbonyl complexes reported here, OUCO and OThCO, are interesting new molecules for several reasons. First, they are formally An(II) complexes, which is a very unusual oxidation state for the actinide elements and is, to our knowledge, an unknown oxidation state for U and Th.[53] Second, the presence of a π-basic oxo ligand, which typically favors high oxidation states, and a π-acidic carbonyl ligand, which generally favors lower oxidation states, presents an interesting contrast between the bonding in two very common ligands within a single molecule. Third, the unusual calculated geometries of these complexes along with their predicted high spin states suggest an unusual combination of bonding effects involving the oxo and carbonyl ligands. To address these issues, we present here a brief discussion of the bonding interactions in OUCO and OThCO.

We will first describe the OUCO molecule. We will consider the bonding interactions that occur when a carbonyl ligand interacts with the frontier orbitals of a UO fragment. This analysis is most easily carried out by assuming a linear geometry, even though we find a bent structure for the molecule. Figure 8 presents an orbital interaction diagram for UO interacting with CO in a linear geometry.

The atomic orbitals of a uranium atom follow the energetic ordering 7s < 5f < 6d. The interaction of an O atom with a U atom will lead to destabilization of the σ and π orbitals. The U 7s, 5fσ, and 6dσ orbitals are thus raised in energy, as are the 5fπ and 6dπ orbitals. When a CO ligand interacts with the UO fragment, donation from the filled CO 5σ orbital leads to further destabilization of the U-based σ orbitals. By contrast, the empty CO 2π orbitals act as acceptor orbitals, stabilizing the U 5fπ and 6dπ orbitals. The predominantly 5fπ MO of linear OUCO, which is actually an admixture of U 5fπ (42%) and U 6dπ (22%), is therefore simultaneously destabilized by O → U π donation and stabilized by U → CO π back-donation. As a consequence, the 5fπ is the lowest energy of the 5f-based MO's, but it is not stabilized sufficiently to isolate it from the rest of the 5f manifold. In addition, the U 7s-based MO, which is destabilized by σ donation from both the oxo and carbonyl ligands, ends up energetically in the midst of the 5f manifold. The relative MO energies are such that linear OUCO has a $^5\Phi$ lowest energy state corresponding to a $(f\pi)^2(s\sigma)^1(f\phi)^1$ configuration.

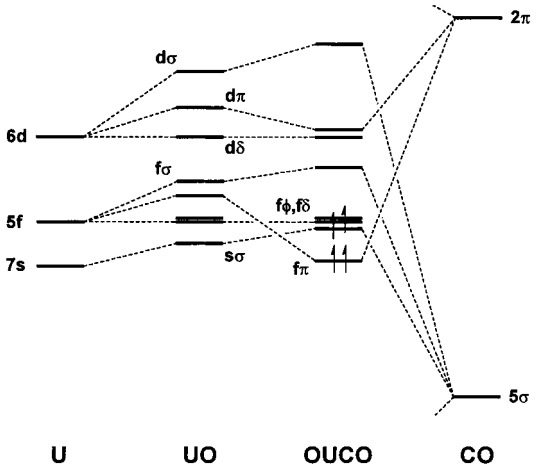

Figure 8. Interaction diagram showing the formation of the molecular orbitals of linear OUCO from the interaction of UO and CO. The molecular orbitals of π, δ, and ϕ symmetry are doubly degenerate. As diagrammed, the linear OUCO molecule is in its $^5\Phi$ lowest energy state.

The back-bonding of the two fπ electrons into the CO 2π orbital would lead to a reduction of the CO stretching frequency, but probably not the ca. 300 cm^{-1} reduction that is observed experimentally. However, the above description of the bonding in linear OUCO leads to the prediction that the molecule would undergo a first-order Renner−Teller distortion to remove the degeneracy of the electron that resides in the fϕ orbitals. By bending the molecule at the U atom, the energy is lowered substantially (0.36 eV). Further, the U → CO back-bonding can be significantly increased upon bending while still preserving the favorable high-spin quintet state because the in-plane CO 2π orbital can now interact with the electron that was in the nonbonding fϕ orbital in the linear geometry. The severe bending of OUCO to its optimized geometry (O−U = 1.828 Å, U−C = 2.259 Å, C−O = 1.174 Å, ∠O−U−C = 113.8°, ∠U−C−O = 179.1°) is therefore seen as a consequence of maximizing the U−CO π interaction while maintaining the high electron exchange stabilization of the quintet state.

The bonding in OThCO differs substantially from that in OUCO for two primary reasons. First, a Th(II) center has only two valence electrons as compared to the four valence electrons present in U(II). The differing electron counts of Th and U can critically influence the electronic structure of small actinide insertion products, as we have previously pointed out in our study of CThO and CUO.[33,34] Second, the energetic ordering of the orbitals in Th is 7s < 6d < 5f, i.e., the 6d orbitals are below the 5f orbitals, and the metal-based electrons are thus expected to occupy the 6d orbitals in preference to the 5f orbitals. Indeed, previous experimental and theoretical studies on tris(cyclopentadienyl) thorium(III) complexes have shown that the single Th-based electron is predominantly 6d in character rather than 5f.[54] The electronic structure of linear OThCO therefore differs from that of OUCO insofar as there are only two metal-based valence electrons and the predomi-

(52) Gedanken, A.; Raz, B.; Jortner, J. *J. Chem. Phys.* 1973, *58*, 1178.
(53) Greenwood, N. N.; Earnshaw, A. *Chemistry of the Elements*, 2nd Ed.; Butterworth-Heinemann: Oxford, UK, 1997.

nantly U 6dπ MO is lower than the predominantly U 5fπ MO. We find that the lowest state of linear OThCO is the $^3\Pi$ state, corresponding to an $(s\sigma)^1(d\pi)^1$ outer configuration. Like linear OUCO, linear OThCO is subject to a first-order Jahn−Teller distortion, and the final optimized geometry of triplet OThCO (O−Th = 1.871 Å, Th−C = 2.488 Å, C−O = 1.161 Å, ∠O−Th−C = 90.8°, ∠Th−C−O = 176.8°) shows bending that is even greater than that in OUCO. This observation is consistent with the participation of Th 6d electrons in OThCO vs U 5f electrons in OUCO and is reminiscent of the situation in the isoelectronic actinyls ThO_2, which is bent, vis-à-vis UO_2^{2+}, which is linear.[55]

The experimental and calculated CO-stretching frequencies in OUCO and OThCO, which are all reduced by about 300 cm^{-1} from that of free CO, indicate extensive π-back-bonding to the CO ligand despite a rather small number of metal-based electrons. In both molecules, the bent structure allows the actinide atom to serve as an efficient "conduit" of electron density from the strongly donating oxo ligand to the CO ligand. In general, the An 6d orbitals interact more strongly with ligands than do the more radially contracted 5f orbitals. Consistent with this notion, the experimental CO-stretching frequencies indicate greater back-bonding in OThCO [ν_{CO} = 1778 cm^{-1} (exptl), 1789 cm^{-1} (calcd)] than in OUCO [ν_{CO} = 1807 cm^{-1} (exptl), 1842 cm^{-1} (calcd)], even though the Th−C bond in OThCO (2.488 Å) is longer than the U−C bond in OUCO (2.259 Å). Indeed, the longer Th−C bond reflects the greater radial extension of the Th 6d orbitals as compared to the U 5f orbitals.

Conclusions

Laser-ablated U and Th atoms react with CO_2 to give OUCO (1806.9, 823.2 cm^{-1}) and OThCO (1778.4 cm^{-1}) as major products, which are identified by isotopic substitution ($^{13}CO_2$, $C^{18}O_2$ and $^{12}CO_2 + {}^{13}CO_2$, $C^{16}O^{18}O + C^{18}O_2$ mixtures), doping with CCl_4 electron trap, and comparison with frequencies from density functional calculations. The insertion reaction is spontaneous as these bands increase on annealing the neon matrix from 4 to 6 K. Further reaction with another CO_2 molecule gives the $O_2An(CO)_2$ product although much more with uranium than thorium. Reaction of the metal cations produces $OUCO^+$ (2073.0, 881.2 cm^{-1}) and $OThCO^+$ (2009.9, 896.4 cm^{-1}) with higher yield in thorium experiments. The $O_2An(CO)_2^-$ anions are observed for both metals again with higher yield in uranium investigations.

Relativistic density functional frequency calculations provide valuable assistance for the identification of new actinide containing molecules. For the OAnCO and $OAnCO^+$ species, the carbonyl modes are fit to 1.9 and 3.2% for U and to 0.6 and 0.4% for Th, and the U−O modes to within 1.4 to 4.4% and one Th−O mode to 2.0%, which is satisfactory for these actinide metal species. Complementary argon matrix experiments give bands red shifted 7−19 cm^{-1}, which are appropriate for these actinide molecules.

The oxocarbonyl complexes OThCO and OUCO are exciting new actinide molecules that combine traditional donor (O) and acceptor (CO) ligands. Both molecules are high spin, are severely bent, and exhibit large An → CO back-bonding. The electronic structure calculations indicate that the metal-based electrons in OThCO are derived from the Th 7s and 6d orbitals, whereas those in OUCO are from the U 7s and 5f orbitals, thus underscoring again some of the basic differences in the structure and bonding in analogous Th and U complexes.

Acknowledgment. We gratefully acknowledge support for this research from the National Science Foundation (Grant CHE 97-00116 to L.A.), from the Division of Chemical Sciences, U.S. Department of Energy (Grant DE-FG02-86ER13529 to B.E.B.), from Los Alamos National Laboratory, and from the Ohio Supercomputer Center and the Environmental Molecular Sciences Laboratory at Pacific Northwest National Laboratory for grants of computer time and preliminary experiments performed by G. P. Kushto.

JA0016699

(54) (a) Kot, W. K.; Shalimoff, G. V.; Edelstein, N. M.; Edelman, M. A.; Lappert, M. F. *J. Am. Chem. Soc*. **1988**, *110*, 986. (b) Bursten, B. E.; Rhodes, L. F.; Strittmatter, R. J. *J. Am. Chem. Soc.* **1989**, *111*, 2756.

(55) Pepper, M.; Bursten, B. E. *Chem. Rev.* **1991**, *91*, 719 and references therein.